Prediction of the Western North Pacific Subtropical High in Summer without Strong ENSO Forcing

Chaofan LI[1,3*], Riyu LU[2,3], and Nick DUNSTONE[4]

1 *Center for Monsoon System Research, Institute of Atmospheric Physics, Chinese Academy of Sciences, Beijing* 100029, *China*

2 *State Key Laboratory of Numerical Modeling for Atmospheric Sciences and Geophysical Fluid Dynamics, Institute of Atmospheric Physics, Chinese Academy of Sciences, Beijing* 100029, *China*

3 *College of Earth and Planetary Sciences, University of Chinese Academy of Sciences, Beijing* 100049, *China*

4 *Met Office Hadley Centre, Exeter* EX1 3PB, *UK*

(Received June 23, 2020; in final form November 17, 2020)

ABSTRACT

The western North Pacific subtropical high (WNPSH) is one of the deterministic predictors of the East Asian summer climate, and a better prediction of the WNPSH favors more reasonable forecast of the East Asian summer climate. This study focuses on seasonal prediction of the WNPSH during neutral summers without strong El Niño–Southern Oscillation (ENSO) forcing, and explores the associated predictable sources, using the one-month lead time retrospective forecasts from the Ensembles-Based Predictions of Climate Changes and Their Impacts (ENSEMBLES) project during 1960–2005. The results indicate that the ENSEMBLES atmosphere–ocean–land coupled models exhibit considerable prediction skill for the WNPSH during neutral summers, with successful reproduction of the WNPSH in the majority of neutral summers. The anomalous WNPSH in neutral summers, which corresponds to cyclonic/anticyclonic anomalies in the lower troposphere, is highly correlated with an east–west dipole local sea surface temperature (SST) distribution over the tropical WNP, suggesting an intimate local air–sea coupling. Further diagnosis of the local SST–rainfall relationship and surface heat flux indicates that the anomalous local SST plays an active role in modulating the variation of the WNPSH during neutral summers, rather than passively responding to the atmospheric change. The local SST anomalies and relevant air–sea coupling over the tropical WNP are reasonably well reproduced in the model predictions, and could act as primary predictable sources of the WNPSH in neutral summers. This could aid in forecasting of the East Asian rainband and associated disaster mitigation planning.

Key words: western North Pacific, subtropical high, seasonal forecast, neutral year, air–sea interaction

Citation: Li, C. F., R. Y. Lu, and N. Dunstone, 2021: Prediction of the western North Pacific subtropical high in summer without strong ENSO forcing. *J. Meteor. Res.*, **35**(1), 101–112, doi: 10.1007/s13351-021-0113-3.

1. Introduction

The western North Pacific subtropical high (WNPSH) is one of the most important components in the seasonal forecast over East Asia, as it closely modulates variations of the East Asian summer climate (e.g., Huang and Sun, 1992; Wang et al., 2000; Lu, 2004). Anomalous location and displacement of the WNPSH are often associated with natural hazards over East Asia, such as persistent drought, flooding, extreme heat, and landfalling typhoons. Thus, knowledge of the predictable sources of the WNPSH and predictability of the WNPSH could be of substantial benefit to disaster mitigation and associated economic planning.

Current atmosphere–ocean coupled forecast systems show good performance in predicting the year-to-year variation of the WNPSH in summer (Lee et al., 2011; Li et al., 2012, 2016; Lu et al., 2012; Kosaka et al., 2013; MacLachlan et al., 2015; Liu et al., 2018). Using the retrospective forecast (hindcast) from the Ensembles-Based

Supported by the National Key Research and Development Program of China (2018YFC1506005), National Natural Science Foundation of China (41775083), and the Second Tibetan Plateau Scientific Expedition and Research (STEP) Program (2019QZKK0102). Nick Dunstone was supported by the UK–China Research and Innovation Partnership Fund through the Met Office Climate Science for Service Partnership (CSSP) China as part of the Newton Fund.

*Corresponding author: lichaofan@mail.iap.ac.cn

Predictions of Climate Changes and Their Impacts (ENSEMBLES) project, Li et al. (2012) pointed out that the WNP summer precipitation and circulation anomalies in the lower troposphere are reliably reproduced by the coupled models, with the predictable sources arising mainly from the air–sea interactions over tropical oceans.

Further exploring the origin of the WNPSH predictability, many studies have found that the air–sea feedback from El Niño–Southern Oscillation (ENSO) evolution is the leading predictor (e.g., Wang et al., 2008; Kosaka et al., 2012; Li et al., 2014). Interannual variation of the WNPSH is closely modulated by ENSO and the associated air–sea interactions over tropical oceans (Wang and Zhang, 2002; Wu et al., 2009; Xie et al., 2016). When an El Niño episode develops around the tropical eastern and central Pacific Ocean, an anomalous anticyclone tends to occur around the Philippine Sea during the El Niño mature winter to the following summer (Wang and Zhang, 2002). Furthermore, anomalous summer circulation over the WNP can also be excited during a developing El Niño phase, due to the strong sea surface temperature (SST)-forced tropical air–sea interactions (Wu et al., 2009). As the dominant mode of interannual climate variability, ENSO is the dominant contribution to the summer predictable sources of the WNPSH.

However, El Niño/La Niña events occur at irregular intervals of two to seven years and weak SST signals appear over the tropical eastern and central Pacific Ocean during the majority of non-El Niño/La Niña years. Identification of the alternative predictable sources/signals of the WNPSH when there is no strong ENSO remains a challenge for forecasters and decision makers. After isolating the ENSO-induced variability by suppressing the SST in a model experiment, Kosaka et al. (2013) suggested that the anomalous WNPSH variation and its meridional teleconnection with the East Asian summer climate exist without ENSO. By exploring the local and remote factors affecting the WNP air–sea coupling through the WNP SST–rainfall relationship, Lu and Lu (2014) pointed out that remote and local SSTs make distinct contributions to formation of the ocean–atmosphere coupled environment over the WNP. Thus, further exploring the local ocean–atmosphere coupling could add value to the predictable sources of the WNP summer climate.

Using the long-time-period (46 yr) hindcast from the ENSEMBLES project, Li et al. (2014) assessed the predictability of the WNPSH associated with different ENSO phases, and found that the ENSEMBLES atmosphere–ocean coupled models show considerable capability in capturing the summer anomalies over the WNP during neutral years without strong ENSO forcing. By recalculating the prediction correlation of neutral summers following Li et al. (2014), as shown in Fig. 1, high prediction skill for lower-tropospheric zonal wind is found along the tropical and subtropical WNP, corresponding to a good description of the WNPSH variation (Fig. 1a). Furthermore, SST and precipitation anomalies around the Maritime Continent and the Philippine Sea are also well reproduced by the models (Figs. 1b, c). This suggests that skillful forecasts of the WNPSH are possible during summers influenced by ENSO neutral conditions.

In this study, we aim to explore the underlying predictable sources of the WNPSH during the summers without strong ENSO forcing. Local ocean–atmosphere coupling, including the local relationship between precipitation and SST and associated local surface flux adjustment, which are often examined for understanding the possible processes of WNP variability (Wu et al., 2006; Ding et al., 2014; Lu and Lu, 2014), are diagnosed here.

The structure of this paper is as follows. Section 2 describes the hindcast systems, data, and methods used in this study. Section 3 shows the performance of models in predicting the WNPSH during neutral summers. Section 4 discusses the possible local ocean–atmosphere coupling processes, including the associated anomalous local SST and surface flux. A summary and discussion are provided in Section 5.

2. Data and methods

2.1 *Datasets*

In this study, we employed the hindcast datasets from the ENSEMBLES project initiated by the European Union (Van Der Linden and Mitchell, 2009). ENSEMBLES contains five fully coupled atmosphere–ocean–land prediction systems, including the models of the ECMWF, the Leibniz Institute of Marine Sciences at Kiel University (IFM-GEOMAR), Météo-France (MF), the UK Met Office system (UKMO), and the Euro-Mediterranean Center for Climate Change (CMCC-INGV). The models include major radiative forcing but no flux adjustments, with the atmospheric (oceanic) resolutions ranging from T63/L19 (2°/L31) to T159/L62 (0.3°–1.4°/L29). Each model has 9 ensemble members, and there are 45 members in total. The hindcasts are performed each summer (JJA: June, July, and August) from 1960 to 2005, initialized on 1 May. This longer hindcast period makes ENSEMBLES the optimal choice for investigating the prediction of neutral summers, via providing more sample data. The model output is calculated as the multi-model ensemble (MME) through a simple composite with equal weight on the 45 members.

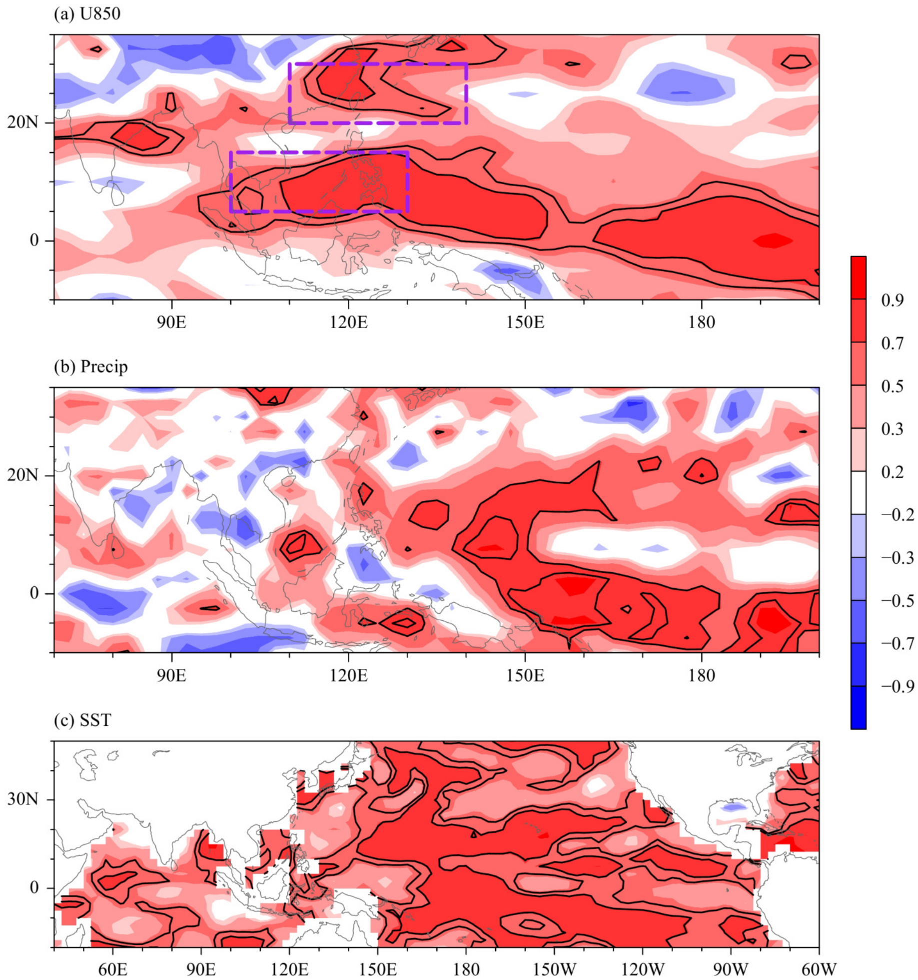

Fig. 1. Prediction skill (shaded; P_Cor) of the (a) 850-hPa zonal wind, (b) precipitation, and (c) SST for ENSO-neutral summers. The ENSO-neutral summers include 1960, 1961, 1962, 1967, 1979, 1980, 1981, 1990, 1993, 2001, 2004, and 2005 (after 1979 for precipitation). The contours represent statistical significance of the prediction correlation at the 0.05 and 0.01 confidence levels. The blue boxes indicate the domains of the WNPSH index.

We used the NCEP/NCAR reanalysis data (Kalnay et al., 1996), NOAA extended reconstructed monthly mean SST version 4 dataset (Huang et al., 2016) during 1960–2005, and the Global Precipitation Climatology Project (GPCP; Adler et al., 2003) during 1979–2005 as proxies for observations, to validate the model hindcasts. In addition, the surface heat flux from the objectively analyzed air–sea fluxes (OAFlux) for global oceans (Yu and Weller, 2007) is used in this study, including longwave (LW) and shortwave (SW) radiation, and latent heat (LH) and sensible heat (SH) fluxes. These flux data are uniformly used from 1984 to 2005, according to the length limit of LW and SW radiative flux data. A positive value indicates downward surface flux that warms the ocean mixed layer and favors a warm SST variation.

2.2 *Methods*

From 1960 to 2005, 12 neutral years are chosen as the neutral summers (1960, 1961, 1962, 1967, 1979, 1980, 1981, 1990, 1993, 2001, 2004, and 2005, as shown in Fig. 2a), by excluding the years related to ENSO developing or decaying phases. An ENSO year is defined when the Niño 3.4 (5°S–5°N, 170°–120°W) index (after removing the 9-yr running mean to obtain the interannual component) is larger than 0.8°C (less than −0.8°C) in winter. The previous (following) summer of the ENSO winter is recognized as an ENSO developing (decaying) summer. The neutral summers are then deduced as the remaining summers after removing the ENSO developing (decaying) summers. The criterion is similar to that in Chou et al. (2003) and Li et al. (2014). We note that the result is robust if other definitions of ENSO events are used.

In this study, the WNPSH index is defined as the difference of the averaged 850-hPa zonal wind anomalies between (5°–15°N, 100°–130°E) and (20°–30°N, 110°–

140°E) (shown in Fig. 1a), following Wang and Fan (1999). A positive WNPSH index corresponds to anomalous cyclonic circulation anomalies over the WNP, suggesting a weakened and northeastward extension of the WNPSH, and vice versa.

To assess the prediction skill of WNPSH in neutral summers, we use the temporal correlation between predicted and observed anomalies (prediction correlation: P_Cor) following Li et al. (2014). The prediction correlation is calculated as the cosine similarity between the prediction and the observation, which is defined as

$$\mathrm{P\_Cor} = \frac{\sum_{i=1}^{n} x_{\mathrm{m}}(i)\, x_{\mathrm{o}}(i)}{\sqrt{\sum_{i=1}^{n} x_{\mathrm{m}}^{2}(i)}\sqrt{\sum_{i=1}^{n} x_{\mathrm{o}}^{2}(i)}}, \quad (1)$$

where n is the number of neutral summers; $x_{\mathrm{m}}(i)$ and $x_{\mathrm{o}}(i)$ are the ith model-predicted and observed summer anomaly, respectively. The resulting similarity ranges from −1 to 1, and a larger value means a high similarity. The significance of this correlation is determined by using Student's t-test.

3. Model performance in neutral summers

Figure 2a shows the observed and model-predicted WNPSH index during all 12 neutral summers. The WNPSH shows large variability during these summers. The corresponding standard deviation is 1.67 m s^{-1} in the observations, which is weaker but comparable to that during all hindcast years (2.06 m s^{-1}). The indices for most neutral summers are positive, with some years larger than one standard deviation. However, some years have negative values, particularly 1993. Compared with the evolution of Niño 3.4 SST index (Fig. 2b), it is inferred that the change of WNPSH anomalies is not related to the

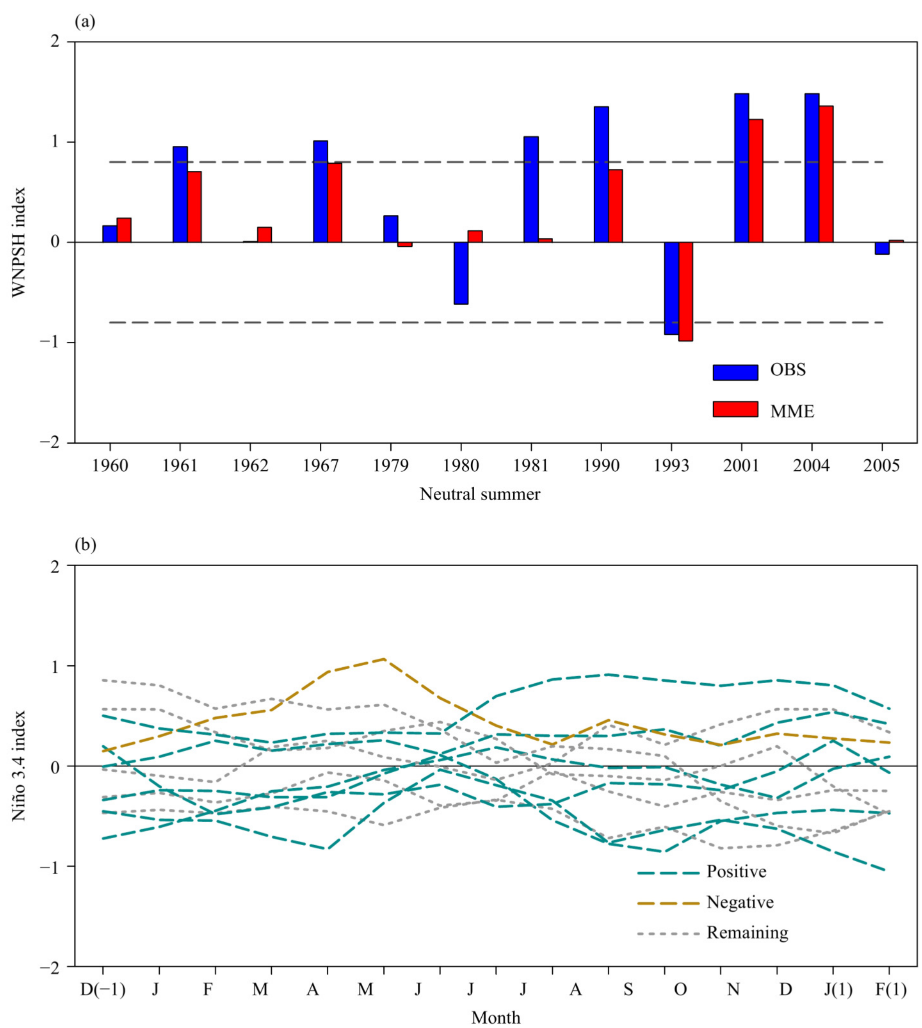

Fig. 2. (a) The normalized WNPSH index for the observations (OBS; blue bar) and model predictions (MME; red bar) during all neutral summers and (b) associated observed evolution of the Niño 3.4 SST index. The positive (negative) years with an observed WNPSH index larger (less) than 0.8 (–0.8) are marked by grey dashed lines in (a) and green (orange) lines in (b) as the significant neutral summers.

ENSO variation during neutral summers, as evolution of the SST anomalies is disorganized over the Niño 3.4 region. The summers with a positive WNPSH index, for example, do not uniformly correspond to La Niña SST anomalies in previous winters or El Niño SST anomalies in the following winters.

The ENSEMBLES models successfully reproduce the WNPSH anomalies during these neutral summers (Fig. 2a). They reasonably predict the anomalies in the majority of summers, and reproduce the large observed variability. The MME prediction correlation is 0.90, which is highly significant and higher than any individual model. The WNPSH is skillfully predicted by all models, with the prediction skill ranging from 0.66 (CMCC-INGV) to 0.74 (MF). The good performance of the models for the WNPSH index is consistent with the significant prediction skill map of lower-tropospheric zonal wind around the WNP (Fig. 1a).

To further explore sources of the variability and skill during neutral summers, we chose the summers with a standardized WNPSH index larger than 0.8 (1961, 1967, 1981, 1990, 2001, and 2004) or less than −0.8 (1993) as the significant neutral years. The anomaly in 1993 is multiplied by −1 in the following analysis to composite with the positive summers.

During these positive summers, apparent cyclonic anomalies occupy the tropical and subtropical WNP in the lower troposphere in the observations (Fig. 3a). Corresponding to these cyclonic anomalies, more (less) rainfall is found over the tropical (subtropical) WNP, showing a meridional teleconnection pattern (Huang and Sun, 1992; Kosaka and Nakamura, 2006). The SST anomalies are relatively weak along the tropical region, but show a dipole SST pattern over the tropical WNP, with positive anomalies around its eastern part and negative anomalies around its western part and northern Indian Ocean (Fig. 3c). Further examining the SST anomalies in individual summers (figures omitted), we found that the negative SST anomalies around the South China Sea and Maritime Continent are mainly contributed by the neutral cases before the late 1970s, while the positive SST anomalies around the western Pacific generally appear in the years after the late 1970s. For the model predictions (Figs. 3b, d), the cyclonic circulation anomalies in the lower troposphere are reproduced, albeit weaker, so are the rainfall and the dipole SST anomalies over the tropical WNP. The regions with these anomalies correspond well to the regions with significant prediction skill (Fig. 1). The negative SST anomalies over the northern Indian Ocean are weaker in the model predictions than in the observations. The above spatial distribution implies a local air–sea coupled mode over the WNP, which exists without strong ENSO forcing. As this is seen in both the observations and the model predictions, the local air–sea coupling may potentially act as a predictable source for the WNPSH during neutral summers. In addition, it is

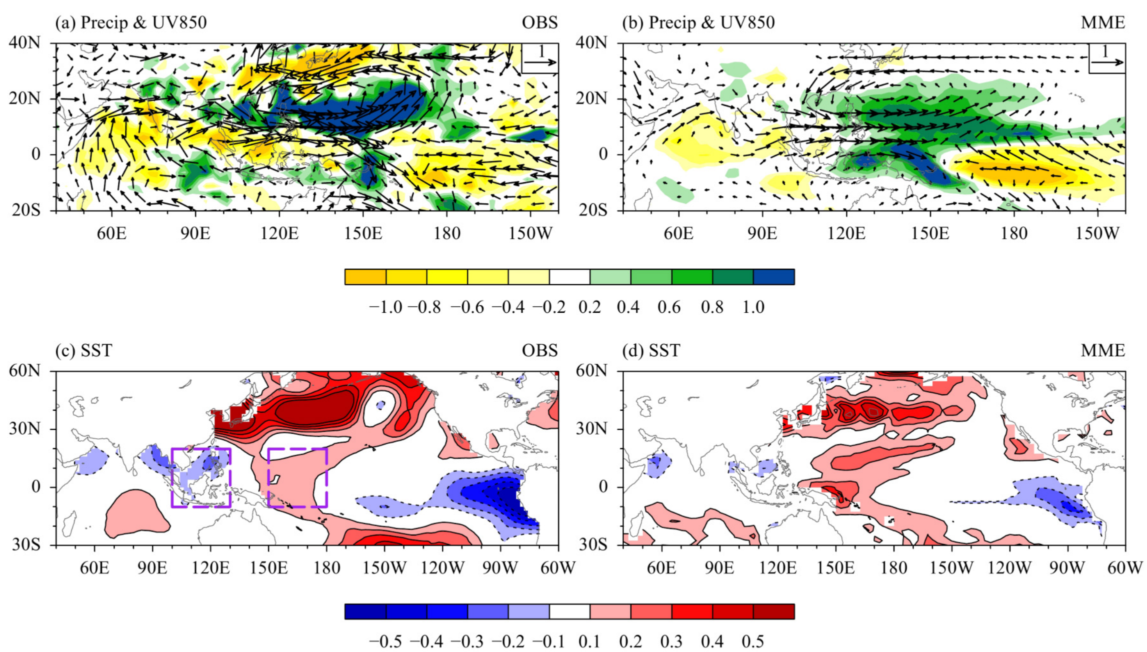

Fig. 3. Composites of the anomalies of (a, b) 850-hPa wind (vector; m s^{-1}) superimposed with precipitation (shading; mm day^{-1}) and (c, d) SST (°C) during the significant neutral summers for (a, c) observations and (b, d) MME predictions. The purple boxes indicate the domains of the dipole SST over the tropical WNP.

worth mentioning that the warm SST anomalies to the east of Japan, which are shown in both the models and the observations, are generally a passive response to the atmosphere variation, as they are associated with negative rainfall anomalies and a negative local SST–rainfall relationship (Wu and Kirtman, 2007).

4. Local air–sea coupling process

4.1 *Dipole SST over the tropical WNP*

To further explore the role of the local SST over the WNP, a dipole SST index is defined as the averaged SST differences between 10°S–20°N, 150°E–180° and 10°S–20°N, 100°–130°E (shown in Fig. 3c), which actually represent the local east–west SST gradient over the WNP. The dipole SST index varies intimately with the WNPSH index in the observations, and the corresponding correlation coefficient is 0.56 during the entire hindcast period (1960–2005).

Figure 4 shows the normalized dipole SST index during the significant neutral summers. It exceeds one standard deviation in many neutral summers, although the anomalies are relatively weak before standardization (Fig. 3c). The SST gradient over the WNP shows a coherent variation with the WNPSH index, with positive anomalies in the majority of summers and negative anomalies in 1993 (Fig. 2a). The gradient is negative in 1981, which is inconsistent with the positive WNPSH index in 1981. This inconsistency corresponds to a failure in prediction of the WNPSH in 1981, where the model reproduces a much weaker WNPSH than the observations (Fig. 2a). The correspondence between the dipole SST over the WNP and the WNPSH further implies the importance of the local air–sea coupling process in seasonal prediction of the WNPSH during neutral summers. The models show excellent performance in predicting the local dipole SST, with a high prediction correlation (0.81).

Further exploring the evolution of this SST gradient (Fig. 5), we found that this positive SST gradient emerges from May and persists mainly in summer, with a consistent variation during most of the neutral years. The anomalies are generally weak in spring, suggesting a warmer tendency from spring to summer. This may imply a seasonable dependence of the local SST anomalies during neutral summers.

An intimate correspondence between the local SST and atmospheric variability over the WNP is found during neutral summers. Previous studies have pointed out that the local SST and lower-tropospheric anomalies over the WNP show a positive feedback, in response to the ENSO forcing (Wang et al., 2000; Wang and Zhang, 2002; Wu et al., 2010). Local positive (negative) SST anomalies over the WNP favor the maintenance of a cyclonic (anticyclonic) anomaly in the lower troposphere via the Rossby wave response. The tropical lower-tropospheric westerly (easterly) associated with the cyclonic (anticyclonic) anomaly can in turn modulate the SST anomalies by surface wind stress. To further test the air–sea coupling, the local correlation between precipitation and SST is diagnosed to determine whether the dipole SST has an active or a passive role in the variation of the WNPSH during neutral summers.

Figure 6 shows scatter diagrams of the standardized SST and precipitation anomalies over the western and eastern WNP for the neutral summers. Given that precipitation data over the ocean are only available from 1979, we examine only the neutral summers after this year. Positive correlations between precipitation and SST anomalies are found over both the western and eastern WNP during these neutral summers. This contrasts with that during all observed summers, in which the precipitation anomalies have a weak negative correlation with the

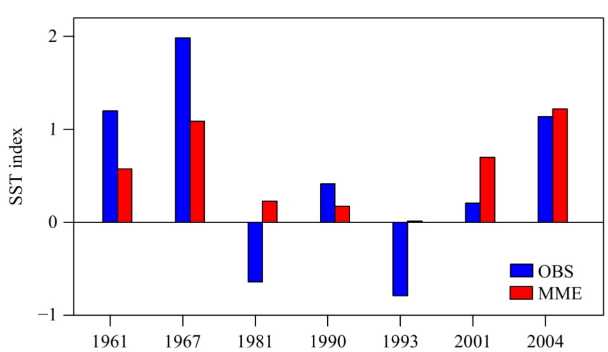

Fig. 4. The normalized dipole SST index over the WNP for the observations (OBS; blue) and the MME predictions (Model; red) during the significant neutral summers. The index is defined by the east–west SST gradient over the WNP, with the domains indicated in Fig. 3c.

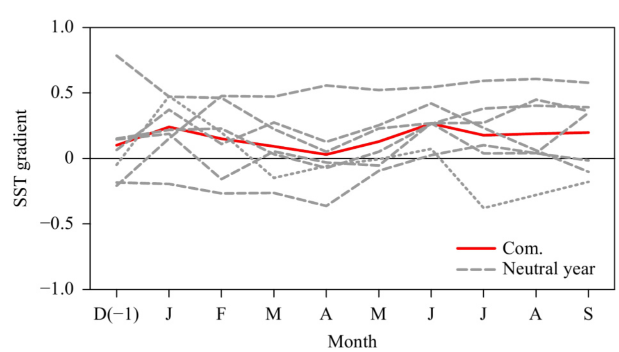

Fig. 5. Seasonal evolution of the observed SST gradient (°C) over the WNP. The anomaly in 1993 (short dashed line) is multiplied by −1 for ease of comparison with the other positive years. Com. denotes composite.

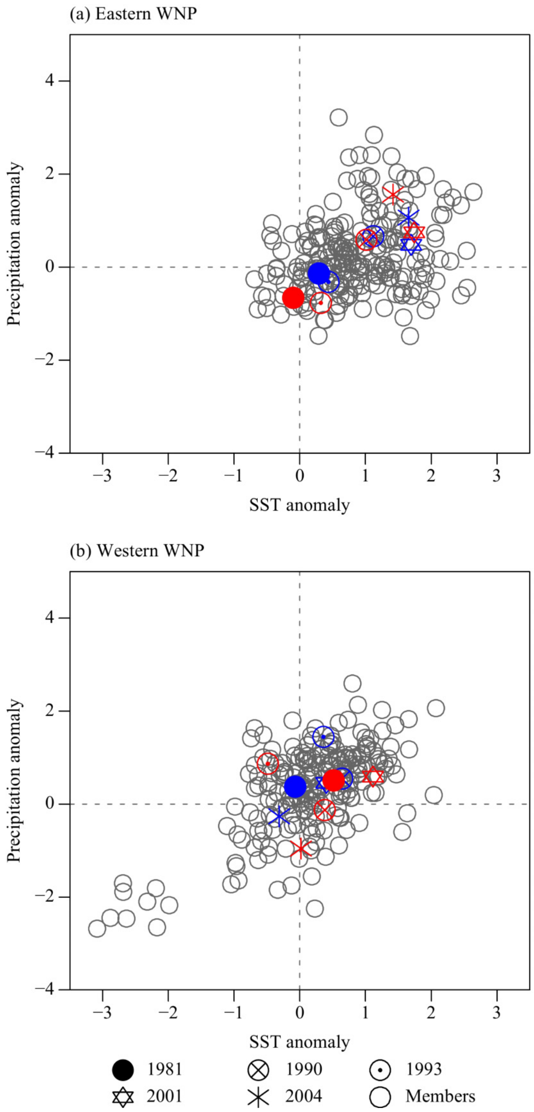

Fig. 6. Scatter diagrams of the standardized SST and precipitation anomalies over the (a) eastern and (b) western WNP for the significant neutral summers after 1979. The blue, red, and grey markers indicate the observations, the MME prediction, and the individual ensemble members, respectively. The domains for the eastern and western WNP are shown in Fig. 3c. The anomaly in 1993 is multiplied by –1. The correlation coefficients between the SST and precipitation anomalies for all these dots are 0.28 in (a) and 0.62 in (b).

underlying SST variation over the WNP (Trenberth and Shea, 2005; Wang et al., 2005; Wu et al., 2006). The positive relationship during the neutral summers implies that the local SST anomalies play a dominant role in the atmospheric variability. Over the eastern WNP, the anomalous warm SST in the majority of the ensemble members corresponds in-phase to a positive precipitation variation (Fig. 6a). The positive SST–rainfall correlation is more evident if we focus on the ensemble mean output, which excludes the influence of internal spread variability. In general, the SST anomalies spread around zero over the western WNP, when taking only the neutral summers after 1979 into consideration. However, a significant positive SST–rainfall correlation is shown here, which is 0.62 among all members in Fig. 6b. The distribution of the SST–rainfall correlation during neutral summers agrees well with previous results in Lu and Lu (2014), in which local SST anomalies over the WNP tend to result in a positive SST–rainfall correlation and the inverse SST–rainfall relationship is associated with the remote forcing, especially the evolution of ENSO. Here, we further point out the model's successful reproduction of this local positive SST–rainfall correlation. In view of the significant prediction skill for SST over the eastern WNP (Fig. 1c), it can potentially act as a primary source for good prediction of the WNPSH during neutral summers.

For the atmospheric component over the WNP during neutral summers, the local convection shows good correspondence with the variation of the WNPSH (Fig. 7). The correlation coefficients between the WNPSH index and the precipitation anomalies over the eastern and western WNP among all the members are 0.61 and −0.31, respectively, both exceeding the 99% confidence level according to Student's *t*-test. Over the eastern WNP, more rainfall from moist adiabatic adjustment favors the maintenance of an anomalous low-level cyclonic circulation, via a Rossby wave response to the local warm SST change (Wang et al., 2000). The anomalous convection over the western WNP, especially that around the Maritime Continent, however, could also modulate the WNPSH variation through an eastward-extended Kelvin wave propagation (Wu et al., 2005; Kosaka et al., 2013). Here, the large number of ensemble members in the model predictions provides ample samples to support the good correspondence among the local SST, precipitation, and WNPSH anomalies during neutral summers.

Compared with the SST anomalies during neutral summers, the remote SST anomalies play a more dominant role in the source of the WNPSH predictability during the ENSO forcing summers. An east–west dipole local SST also appears over the WNP during ENSO decaying and developing summers (Fig. 7 in Li et al., 2014). However, the local SST–rainfall relationship is generally negative during ENSO decaying summers (Wu et al., 2009), suggesting that in general, the SST anomalies passively respond to the atmospheric variations, which are forced and maintained by the ENSO signals from the previous seasons (Wang et al., 2000) and the tropical Indian Ocean SST anomalies (Xie et al., 2009). During ENSO developing summers, in contrast, a positive SST–rainfall relationship is found around the Maritime

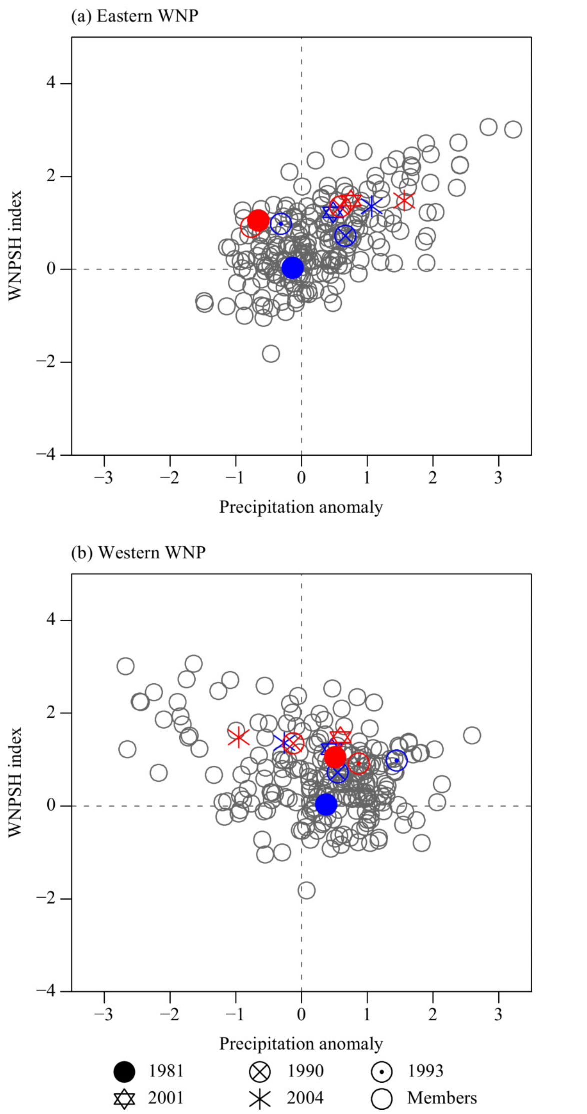

Fig. 7. As in Fig. 6, but for the standardized WNPSH index and precipitation anomalies over the (a) eastern and (b) western WNP. The correlation coefficients between the WHPSH index and precipitation anomalies for all these dots are 0.61 in (a) and –0.31 in (b).

Continent (Wu et al., 2009), which could add value to the predictability of the WNPSH. However, the significant SST anomalies around the tropical eastern Pacific related to the developing ENSO play a more dominant role in the source of the WNPSH predictability, and also contribute to the SST anomalies around the Maritime Continent (Wang and Zhang, 2002).

4.2 *Surface flux*

Figure 8 shows spatial distributions of the surface fluxes over the WNP in the observations and model predictions during neutral summers. In the observations, positive LW radiation flux anomalies appear over a large region of the WNP, implying that the downward LW flux makes a positive (negative) contribution and favors warmer SSTs over the eastern (western) WNP (Fig. 3c). In contrast, the anomalous SW and LH fluxes contribute negatively (positively) to the eastern (western) SST variation, with negative anomalies over most regions of the WNP. The negative SW anomalies correspond to the positive precipitation anomalies over the tropical WNP (Fig. 3a), favoring increased cloud cover but not favorable for the maintenance of warm SSTs over the eastern WNP. The negative LH flux is closely related to the anomalous cyclonic lower-tropospheric circulation (Fig. 3a), which favors more evaporation and a cooling effect on the local SST. Relatively, the SH flux over the WNP is much weaker than the other flux anomalies, suggesting a weak contribution to summer SST anomalies. In general, the model predictions reproduce the distributions of surface flux anomalies over the WNP, especially the positive LW and negative SW anomalies around the Philippine Sea. This good performance suggests that the coupled models have a certain capability in capturing the effect of atmospheric feedback on the surface ocean variability.

Owing to contributions of the SW and LH fluxes, the total surface flux anomalies over the eastern WNP around the Philippine Sea are negative (Fig. 9). The averaged flux anomalies averaged over the eastern WNP (10°S–20°N, 150°E–180°) are −9.06 and −6.94 W m^{-2} for the observations and the model predictions, respectively. By comparison, the spatial distribution of the surface flux anomalies shows a large contrast to the SST distribution over the WNP, but more closely resembles the atmospheric components (Fig. 3). This indicates that these surface flux anomalies are not favorable for the maintenance of local SST anomalies over the WNP. The local SST anomalies dominate the air–sea interactions during neutral summers, rather than passively responding to the atmospheric variations. The ENSEMBLES coupled models demonstrate a good capability in describing these local air–sea interactions, especially the local SST anomalies, and thus contribute to the considerable prediction skill of the WNPSH during neutral summers.

5. Summary and discussion

As the dominant interannual climate variability, ENSO acts as the leading predictor for the East Asian summer monsoon. Nevertheless, there still exist many neutral years in which the associated seasonal forecast cannot rely on the ENSO evolution and associated air–sea interactions. Interannual variation of the WNPSH, which links tropical signals with the East Asian summer cli-

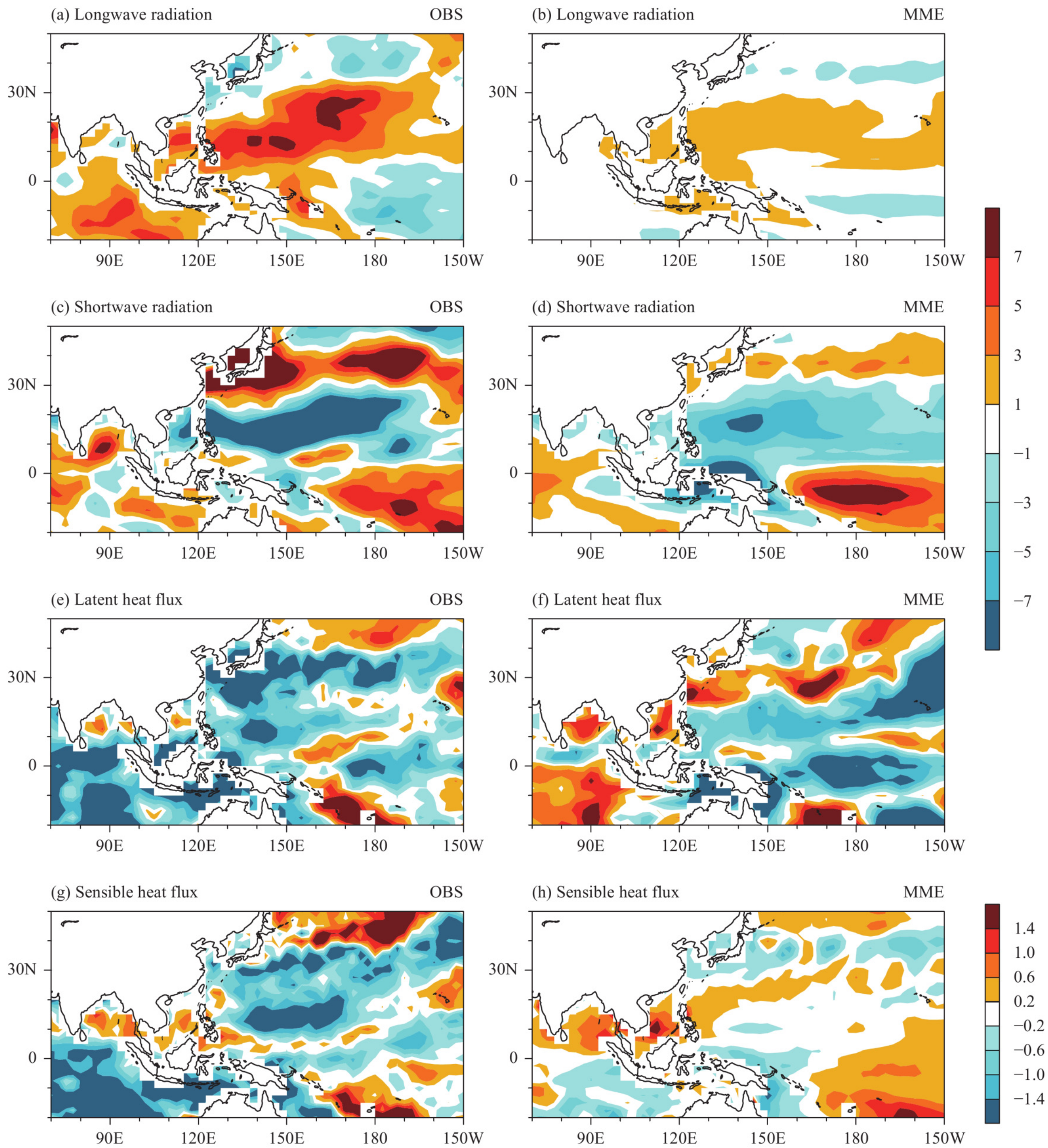

Fig. 8. Composites of the surface fluxes from the observations (left panels) and MME predictions (right panels) during the significant neutral summers, including (a, b) longwave (LW) radiation, (c, d) shortwave (SW) radiation, (e, f) latent heat (LH) flux, and (g, h) sensible heat (SH) flux. The units are W m^{-2} and positive values indicate downward flux.

mate, directly modulates the East Asian summer monsoon. In this study, we assess the performance of the ENSEMBLES coupled models in predicting the WNPSH during neutral summers without strong ENSO forcing, and further identify the predictable sources from the local air–sea coupling process. The hindcasts of the ENSEMBLES project initialized on 1 May during 1960–2005 are used here. This long hindcast period is needed to provide a sufficient number of neutral summer cases.

Considerable prediction capability for the WNPSH index and associated summer anomalies is demonstrated by the models. The prediction correlation of the WNPSH index reaches 0.90 among the 12 neutral summers in the MME output. Without strong ENSO forcing, the WNPSH also shows large interannual variability, corresponding to anomalous cyclonic/anticyclonic circulation in the lower troposphere, precipitation anomalies, and an east–west dipole SST distribution over the tropical WNP. These features are successfully captured by the model predictions.

The dipole SST distribution over the tropical WNP with an east–west SST gradient is positively related to

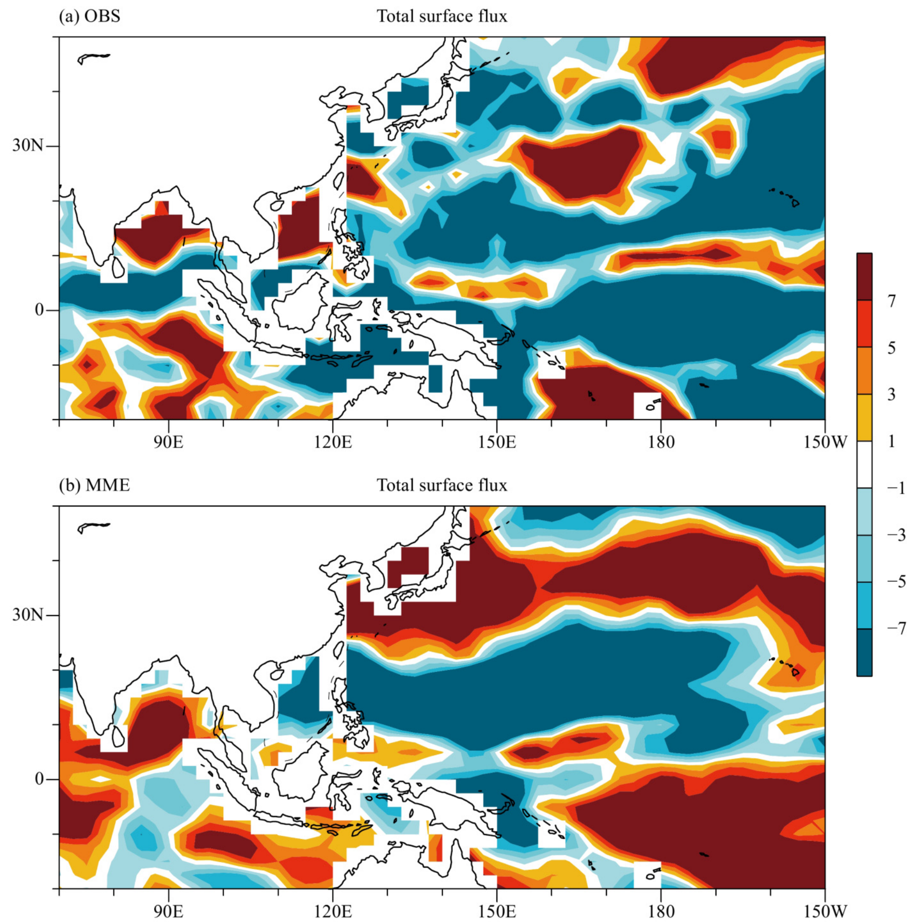

Fig. 9. As in Fig. 8, but for the total surface flux anomalies.

the local precipitation anomalies. Over the tropical eastern WNP, on the one hand, the positive SST anomalies tend to induce enhanced local precipitation. The surface flux anomalies over this region, especially the SW and LH fluxes, are negative during neutral summers and cannot support the maintenance of these positive SST anomalies. This suggests that the anomalous SSTs around the tropical eastern Pacific may dominate the local atmospheric variations. The models reasonably describe the local air–sea coupling process over the WNP, including a high prediction correlation of SST anomalies, the positive SST–rainfall relationship, and the surface flux anomalies. These good performances contribute to the considerable prediction skill of the WNPSH during neutral summers. Over the tropical western WNP, on the other hand, the significant positive local SST–rainfall relationship also implies the importance of local SST change, although the anomalies are not uniformly negative after the late 1970s.

This study focuses on the hindcasts with one-month lead time that are initialized in May. We also assess the prediction skill of the hindcasts with longer lead times in ENSEMBLES, and find that the high WNPSH prediction skill could also be achieved with a four-month lead time (initialized on 1 February). The prediction correlation between the MME and the observations for the WNPSH index is 0.86. The good predictions achieved here indicate that the coupled model output for the WNPSH is reliable during neutral summers, and could act as a good reference for forecasters and decision makers, in forecasting the position and intensity of the East Asian rainband, and for disaster mitigation of the associated floods, droughts, and landfalling tropical cyclones. Unfortunately, the skill turns relatively low for the predictions at seven-month lead time (initialized on the previous 1 November). The corresponding prediction correlation of the WNPSH index is 0.43.

In this study, we emphasize the importance of local SSTs to the high WNPSH predictability during ENSO-neutral summers. While the anomalous local SSTs over the WNP play an active role in the maintenance of the anomalous WNPSH, we have not explored the causes of the anomalous SSTs themselves, and this would be interesting future work. In addition, it is intriguing that the

WNPSH index is generally positive in the neutral summers shown here, showing an anomalous lower-tropospheric cyclone over the tropical WNP (Figs. 2a, 3a). It can be argued that this may arise from an insufficient number of samples of neutral summers. However, this situation also appears in the model predictions, which include plenty of ensemble members and could offset the impact of insufficient samples. For a better understanding of these positive anomalies in neutral summers, future studies focusing on the asymmetric features of the WNPSH variation are needed, including its nonlinear response to ENSO evolution.

This study mainly discusses the contributions of the tropical SST to the WNPSH during ENSO-neutral summers. The results are valid in both the observations and the model simulations. Some other factors, such as the midlatitude wave disturbances (e.g., Lu et al., 2002; Hong and Lu, 2016; Li et al., 2017), monsoon diabatic heating (e.g., Rodwell and Hoskins, 2001; Kosaka and Nakamura, 2006), and land–sea thermal contrast (Wu and Liu, 2003; Miyasaka and Nakamura, 2005), have been proposed to modulate the formulation and maintenance of the WNPSH. These factors may vary from case to case among the neutral summers and are not discussed here. In addition, the models in the ENSEMBLES project used here are relatively old, even though this project has provided a quite long hindcast. We would expect a similar or better prediction for the WNPSH during neutral summers if current coupled models with a considerably higher resolution were used.

Acknowledgments. The ENSEMBLES data used in this work are funded by the EU FP6 Integrated Project ENSEMBLES (Contract Number 505539), whose support to this study is gratefully acknowledged.

REFERENCES

Adler, R. F., G. J. Huffman, A. Chang, et al., 2003: The Version-2 Global Precipitation Climatology Project (GPCP) monthly precipitation analysis (1979–present). *J. Hydrometeor.*, **4**, 1147–1167, doi: 10.1175/1525-7541(2003)004<1147:TVGP-CP>2.0.CO;2.

Chou, C., T. Y. Tu, and Y. J. Yu, 2003: Interannual variability of the western North Pacific summer monsoon: Differences between ENSO and non-ENSO years. *J. Climate*, **16**, 2275–2287, doi: 10.1175/2761.1.

Ding, H., R. J. Greatbatch, W. Park, et al., 2014: The variability of the East Asian summer monsoon and its relationship to ENSO in a partially coupled climate model. *Climate Dyn.*, **42**, 367–379, doi: 10.1007/s00382-012-1642-3.

Hong, X. W., and R. Y. Lu, 2016: The meridional displacement of the summer Asian jet, Silk Road pattern, and tropical SST anomalies. *J. Climate*, **29**, 3753–3766, doi: 10.1175/jcli-d-15-0541.1.

Huang, B. Y., P. W. Thorne, T. M. Smith, et al., 2016: Further exploring and quantifying uncertainties for extended reconstructed sea surface temperature (ERSST) version 4 (v4). *J. Climate*, **29**, 3119–3142, doi: 10.1175/jcli-d-15-0430.1.

Huang, R. H., and F. Y. Sun, 1992: Impacts of the tropical western Pacific on the East Asian summer monsoon. *J. Meteor. Soc. Japan*, **70**, 243–256, doi: 10.2151/jmsj1965.70.1B_243.

Kalnay, E., M. Kanamitsu, R. Kistler, et al., 1996: The NCEP/NCAR 40-year reanalysis project. *Bull. Amer. Meteor. Soc.*, **77**, 437–472, doi: 10.1175/1520-0477(1996)077<0437:TNYRP>2.0.CO;2.

Kosaka, Y., and H. Nakamura, 2006: Structure and dynamics of the summertime Pacific–Japan teleconnection pattern. *Quart. J. Roy. Meteor. Soc.*, **132**, 2009–2030, doi: 10.1256/qj.05.204.

Kosaka, Y., J. S. Chowdary, S.-P. Xie, et al., 2012: Limitations of seasonal predictability for summer climate over East Asia and the northwestern Pacific. *J. Climate*, **25**, 7574–7589, doi: 10.1175/JCLI-D-12-00009.1.

Kosaka, Y., S.-P. Xie, N.-C. Lau, et al., 2013: Origin of seasonal predictability for summer climate over the Northwestern Pacific. *Proc. Natl. Acad. Sci. USA*, **110**, 7574–7579, doi: 10.1073/pnas.1215582110.

Lee, S. S., J. Y. Lee, K. J. Ha, et al., 2011: Deficiencies and possibilities for long-lead coupled climate prediction of the western North Pacific–East Asian summer monsoon. *Climate Dyn.*, **36**, 1173–1188, doi: 10.1007/s00382-010-0832-0.

Li, C. F., R. Y. Lu, and B. W. Dong, 2012: Predictability of the western North Pacific summer climate demonstrated by the coupled models of ENSEMBLES. *Climate Dyn.*, **39**, 329–346, doi: 10.1007/s00382-011-1274-z.

Li, C. F., R. Y. Lu, and B. W. Dong, 2014: Predictability of the western North Pacific summer climate associated with different ENSO phases by ENSEMBLES multi-model seasonal forecasts. *Climate Dyn.*, **43**, 1829–1845, doi: 10.1007/s00382-013-2010-7.

Li, C. F., R. Y. Lu, and B. W. Dong, 2016: Interdecadal changes on the seasonal prediction of the western North Pacific summer climate around the late 1970s and early 1990s. *Climate Dyn.*, **46**, 2435–2448, doi: 10.1007/s00382-015-2711-1.

Li, C. F., W. Chen, X. W. Hong, et al., 2017: Why was the strengthening of rainfall in summer over the Yangtze River valley in 2016 less pronounced than that in 1998 under similar preceding El Niño events?—Role of midlatitude circulation in August. *Adv. Atmos. Sci.*, **34**, 1290–1300, doi: 10.1007/s00376-017-7003-8.

Liu, Y., H.-L. Ren, A. A. Scaife, et al., 2018: Evaluation and statistical downscaling of East Asian summer monsoon forecasting in BCC and MOHC seasonal prediction systems. *Quart. J. Roy. Meteor. Soc.*, **144**, 2798–2811, doi: 10.1002/qj.3405.

Lu, R. Y., 2004: Associations among the components of the East Asian summer monsoon system in the meridional direction. *J. Meteor. Soc. Japan*, **82**, 155–165, doi: 10.2151/jmsj.82.155.

Lu, R.-Y., and S. Lu, 2014: Local and remote factors affecting the SST–precipitation relationship over the western North Pacific during summer. *J. Climate*, **27**, 5132–5147, doi: 10.1175/JCLI-D-13-00510.1.

Lu, R.-Y., J.-H. Oh, and B.-J. Kim, 2002: A teleconnection pattern in upper-level meridional wind over the North African and Eurasian continent in summer. *Tellus A: Dyn. Meteor. Oceanogr.*, **54**, 44–55, doi: 10.1034/j.1600-0870.2002.00248.x.

Lu, R.-Y., C.-F. Li, S. H. Yang, et al., 2012: The coupled model predictability of the western North Pacific summer monsoon with different leading times. *Atmos. Ocean. Sci. Lett.*, **5**, 219–224, doi: 10.1080/16742834.2012.11447000.

MacLachlan, C., A. Arribas, K. A. Peterson, et al., 2015: Global Seasonal forecast system version 5 (GloSea5): A high-resolution seasonal forecast system. *Quart. J. Roy. Meteor. Soc.*, **141**, 1072–1084, doi: 10.1002/qj.2396.

Miyasaka, T., and H. Nakamura, 2005: Structure and formation mechanisms of the Northern Hemisphere summertime subtropical highs. *J. Climate*, **18**, 5046–5065, doi: 10.1175/jcli3599.1.

Rodwell, M. J., and B. J. Hoskins, 2001: Subtropical anticyclones and summer monsoons. *J. Climate*, **14**, 3192–3211, doi: 10.1175/1520-0442(2001)014<3192:SAASM>2.0.CO;2.

Trenberth, K. E., and D. J. Shea, 2005: Relationships between precipitation and surface temperature. *Geophys. Res. Lett.*, **32**, L14703, doi: 10.1029/2005GL022760.

Van Der Linden, P., and J. F. B. Mitchell, 2009: ENSEMBLES: Climate Change and Its Impacts: Summary of Research and Results from the ENSEMBLES Project. Met Office Hadley Centre, UK, 160 pp.

Wang, B., and Z. Fan, 1999: Choice of South Asian summer monsoon indices. *Bull. Amer. Meteor. Soc.*, **80**, 629–638, doi: 10.1175/1520-0477(1999)080<0629:COSASM>2.0.CO;2.

Wang, B., and Q. Zhang, 2002: Pacific–East Asian teleconnection. Part Ⅱ: How the Philippine sea anomalous anticyclone is established during El Niño development. *J. Climate*, **15**, 3252–3265, doi: 10.1175/1520-0442(2002)015<3252:PEATPI>2.0.CO;2.

Wang, B., R. G. Wu, and X. H. Fu, 2000: Pacific–East Asian teleconnection: How does ENSO affect East Asian climate? *J. Climate*, **13**, 1517–1536, doi: 10.1175/1520-0442(2000)013<1517:PEATHD>2.0.CO;2.

Wang, B., Q. H. Ding, X. H. Fu, et al., 2005: Fundamental challenge in simulation and prediction of summer monsoon rainfall. *Geophys. Res. Lett.*, **32**, L15711, doi: 10.1029/2005GL022734.

Wang, B., J.-Y. Lee, I.-S. Kang, et al., 2008: How accurately do coupled climate models predict the leading modes of Asian-Australian monsoon interannual variability? *Climate Dyn.*, **30**, 605–619, doi: 10.1007/s00382-007-0310-5.

Wu, B., T. J. Zhou, and T. Li, 2009: Contrast of rainfall–SST relationships in the western North Pacific between the ENSO-developing and ENSO-decaying summers. *J. Climate*, **22**, 4398–4405, doi: 10.1175/2009JCLI2648.1.

Wu, B., T. Li, and T. J. Zhou, 2010: Relative contributions of the Indian Ocean and local SST anomalies to the maintenance of the western North Pacific anomalous anticyclone during the El Niño decaying summer. *J. Climate*, **23**, 2974–2986, doi: 10.1175/2010jcli3300.1.

Wu, G. X., and Y. M. Liu, 2003: Summertime quadruplet heating pattern in the subtropics and the associated atmospheric circulation. *Geophys. Res. Lett.*, **30**, 1201, doi: 10.1029/2002GL016209.

Wu, R. G., and B. P. Kirtman, 2007: Regimes of seasonal air–sea interaction and implications for performance of forced simulations. *Climate Dyn.*, **29**, 393–410, doi: 10.1007/s00382-007-0246-9.

Wu, R. G., J. L. Kinter Ⅲ, and B. P. Kirtman, 2005: Discrepancy of interdecadal changes in the Asian region among the NCEP–NCAR reanalysis, objective analyses, and observations. *J. Climate*, **18**, 3048–3067, doi: 10.1175/jcli3465.1.

Wu, R. G., B. P. Kirtman, and K. Pegion, 2006: Local air–sea relationship in observations and model simulations. *J. Climate*, **19**, 4914–4932, doi: 10.1175/JCLI3904.1.

Xie, S.-P., K. M. Hu, J. Hafner, et al., 2009: Indian Ocean capacitor effect on Indo-western Pacific climate during the summer following El Niño. *J. Climate*, **22**, 730–747, doi: 10.1175/2008JCLI2544.1.

Xie, S.-P., Y. Kosaka, Y. Du, et al., 2016: Indo-western Pacific ocean capacitor and coherent climate anomalies in post-ENSO summer: A review. *Adv. Atmos. Sci.*, **33**, 411–432, doi: 10.1007/s00376-015-5192-6.

Yu, L. S., and R. A. Weller, 2007: Objectively analyzed air–sea heat fluxes for the global ice-free oceans (1981–2005). *Bull. Amer. Meteor. Soc.*, **88**, 527–540, doi: 10.1175/bams-88-4-527.

Tech & Copy Editor: Lan YI